EFFECT OF LAYER CHARGE ON THE SWELLING OF Na^+, K^+, AND Ca^{2+} MONTMORILLONITES: DFT AND MOLECULAR DYNAMICS STUDIES

ANNIINA SEPPÄLÄ [a], EINI PUHAKKA [b] AND MARKUS OLIN [a]

[a] VTT Technical Research Centre of Finland Ltd, P.O. Box 1000, FI-02044 VTT, Finland

[b] Laboratory of Radiochemistry, Department of Chemistry, P.O. Box 55, FI-00014 UNIVERSITY OF HELSINKI, Finland

ABSTRACT: The swelling and cation exchange properties of montmorillonite mineral are fundamental in a wide range of applications ranging from nanocomposites to catalytic cracking of hydrocarbons. The swelling results from multiple factors and, though widely studied, information on the effects of one factor at a time is lacking. In this study, density functional theory (DFT) calculations were used to obtain atomic level information on the swelling of montmorillonite. Molecular dynamics (MD) was used to investigate the swelling properties of montmorillonites with different layer charges and interlayer cationic compositions. MD calculations, with CLAYFF force field, consider three layer charges (-1.0 e, -0.66 e and -0.5 e per unit cell) arising from octahedral substitutions and interlayer counterions of Na, K and Ca. The obtained swelling

curves showed that smaller layer charge results in greater swelling but the type of the interlayer cation also has an effect. It was also seen that DFT calculations predict larger d-values than MD. The formation of 1, 2 and 3 water molecular layers in the interlayer spaces was observed. Last, the data from MD calculations was used to predict the self-diffusion coefficients of interlayer water and cations in different montmorillonites and in general the coefficient increased with increasing water content and with decreasing layer charge.

INTRODUCTION

Smectites are 2:1 -layered swelling clay minerals where the layers are formed of two tetrahedral silicate sheets sandwiching an octahedral aluminum sheet. These negatively charged layers are stacked together with a space for water and charge compensating cations in between. Smectites have the ability to adsorb water into the interlayer spaces and to change the cationic composition. (Brigatti et al., 2006, Velde & Meunier, 2008)

The properties of smectites are under extensive study due to their important role in a wide variety of technological and biochemical applications such as fluid filtration, catalytic processes (Murray, 2000) and the disposal of spent nuclear fuel (Dohrmann et al., 2013). In the concept of geological disposal of nuclear waste a multi barrier system is planned to prevent/retard the release of

radionuclides into biosphere. One of these barrier materials is bentonite clay which main component is a smectite group mineral, montmorillonite. The retardation of radionuclides is mainly based on diffusional transport and sorption on solid mineral surfaces. Like smectites, bentonite swells in contact with water thus blocking transport pathways.

Montmorillonite is a very fine-grained and mechanically stable mineral which is characterized by the amount of layer charge (e/unit cell) and the location of the charge sites, tetrahedral and/or octahedral sheet. Its swelling and cation exchange properties also depend on solution properties like pH, ionic strength and ligands.

Analysis of crystalline properties of clays have been very challenging, but nowadays isotopic difference neutron diffraction and molecular modelling techniques have made it possible to study the interlayer structures of clays and the effect of hydration on the structure (Sposito et al., 1999). In sorption studies, molecular modelling has typically been used in connection with surface characterization such as X-ray photoelectron spectroscopy by Ebina et al. (1999) and extended X-ray absorption fine structure by Hattori et al. (2009). Also, relation between atomistic phenomena and surface complexation modelling has been formulated by Wesolowski et al. (2009). Quantum mechanics (QM) techniques have been used to study e.g. clay-cation (Ren et al., 2012, Tribe et al., 2012) and clay-cation-water (Chatterjee et al., 1999, Sposito et al., 1999)

interactions. Multiscale approach including QM, molecular dynamics (MD) and mesoscopic simulations was presented by Rotenberg et al. (2014). They emphasized the challenge to describe phenomena with different length and time scales in clay studies. However, the benefits of the use of molecular modelling are evident, because the understanding of the chemical reactions requires that the description of the electron structure of the system and the dependence of the thermodynamics as a function of time is known.

MD is used to study larger and more complex systems as compared to QM, e.g. to evaluate equilibrium and transport properties that cannot be calculated analytically (Tambach et al. 2004, Tao et al., 2010). While these properties are determined in the microscopic i.e. atomistic level, they are linked to the macroscopic properties of the bulk system through thermodynamics and statistical mechanics. In this work, QM and MD simulations are performed in order to study the effect of layer charge on montmorillonite's swelling properties. Although the swelling of montmorillonite has been widely studied by molecular modelling, the structures used in these studies vary e.g. substitutions present in different sites (tetrahedral and/or octahedral), different layer charges and different cations (all of which are thought to have an effect on the swelling properties). While considering the effect of layer charge on montmorillonite’s swelling, comparing results from different sources increases the number of

variables and, thus, leads to uncertainty in the comparison. In this work, the layer charge arises from octahedral substitutions alone and the same structures are applied for different cations, which makes the comparison of the results more reliable. In addition, two different molecular modelling methods (QM and MD) are applied to the same structures, making the comparison of the methods straightforward. The QM simulations are performed for a tridimensional periodic system, and MD simulations for a rectangular simulation box containing one clay lamellae and the interlayer with water and cations. The optimized mineral structures defined by the QM methods are utilized in MD simulations. The results from the small scale system QM calculations are compared to those from the slightly larger scale system MD calculations. For the MD simulations, the simulation box was constructed large enough to describe specific chemical interactions of the system in order to perform comparison between different types of montmorillonites. With using larger systems, e.g. bending of clay lamella can prohibit the detection of nanolevel phenomena.

METHODS

Montmorillonite structure

The basic montmorillonite building block is composed of a 2:1 structure with an octahedral (O) sheet sandwiched between two tetrahedral (T) sheets (Viviani

et al., 2002). These sheets stack together to form layers with a characteristic repeat distance between the TOT layers, and which carry a net negative charge. The general unit cell formula for Mg-substituted montmorillonite where the substitutions, i.e. charge sites, occur only in the octahedral sheet is

$$Si_8(Al_{4-x}Mg_x)O_{20}(OH)_4M^{k+}_{x/k} \cdot nH_2O \qquad (1)$$

where M is alkali or alkali earth metal cation (exchangeable cation, here Na^+ , K^+ or Ca^{2+}) and x= 0.4-1.2. Because the number of charge sites in the tetrahedral sheet is small compared to the number of sites in the octahedral sheet (Rowe et al., 1997), no tetrahedral substitutions are present in our small scale calculations. The structure repeats C2/m symmetry, and experimental lattice parameters are a = 518 pm, b = 897 pm, c = 995 pm, $\alpha = \gamma = 90.0°$ and $\beta = 99.5°$ without water molecules in the interlayer space between the TOT layers.

Quantum mechanics

In order to perform reliable MD calculations, accurate crystal structures of pure montmorillonites are needed for starting points of the calculations. In this study, the optimized unit cell structures were determined from QM for Na-, K- and Ca-montmorillonites. As a starting point for QM calculations, experimental atomic coordinates defined by Tsipursky and Drits (1984) for K-smectite were used. The calculations were performed with the density functional CASTEP

(CAmbridge Serial Total Energy Package by Clark et al., 2005) code implemented into Materials Studio versions 6.0 (Accelrys, 2011) and 7.0 (Accelrys, 2013).

Optimization of the unit cell of K-montmorillonite was done using different exchange-correlation energy potentials, pseudopotentials and kinetic cut-off energy values in order to validate the results compared to experimental values. The exchange-correlation was described with generalized gradient approximation GGA-PBE or GGA-PW91. In these calculations, the total electronic energy and overall electronic density distribution were solved in order to define the energetically stable montmorillonite structures (Leach, 2001). As a compromise between the accuracy and computational time of calculations, the ultrasoft pseudopotentials (Table 1) were used for each element, and the kinetic cut-off energy for a plane wave expansion of the wave function was 310 eV.

Optimizations of the unit cells of Na- and Ca-montmorillonites were done using only GGA-PBE approximation. The pseudopotentials are presented in Table 1, and the kinetic cut-off energy for a plane wave expansion of the wave function was 310 eV like in the case of K-montmorillonite.

The optimized unit cells were used to construct model structures (1x3x1 unit cells) for MD simulations. The model structures were reoptimized using GGA-PBE approximation with the pseudopotentials presented in Table 1. For oxygen

and silicon, O_00PBE.usp and Si_00PBE.usp potentials were used. In these calculations, the kinetic cut-off energy for a plane wave expansion of the wave function was 370 eV.

The 1x3x1 model structures were utilized to study enlargement of the montmorillonite structure as a function of water insertion into the interlayer space of montmorillonites. Optimization of the model structures with different water content was done using GGA-PW91 approximation. GGA-PW91 gives better description of the system, and calculations achieve convergence faster than using GGA-PBE. Further, the GGA-PBE overestimates the thickness of the interlayer space for larger systems, because it cannot describe energy states of the system correctly. Calculations were performed using the pseudopotentials presented in Table 1. The kinetic cut-off energy for a plane wave expansion of the wave function was 370 eV.

Hydration of cations was investigated using the density functional DMol3 code implemented into Materials Studio version 7.0 (Accelrys, 2013). Coordination sphere of cations (Na^+, K^+ and Ca^{2+}) was optimized using GGA-PW91 approximation with DNP basis set and DFT based semi-core pseudopotentials. Hydration energies were calculated as a difference between the total energy of a hydrated cation and the total energies of a non-hydrated cation and water molecules.

Table 1. Pseudopotentials used in QM calculations.

	GGA-PBE	GGA-PW91
Al	Al_00PBE.usp	Al_00PBE.usp
Ca	Ca_00PBE.usp	Ca_00PBE.usp
H	H_00PBE.usp	H_00PBE.usp
K	K_00PBE.usp	K_00PBE.usp
Mg	Mg_00.usp	Mg_00PW91.usp
Na	Na_00PBE.usp	Na_00PBE.usp
O	O_00PBE.usp	O_00PBE.usp
	O_soft00.usp	
Si	Si_00PBE.usp	Si_00PBE.usp
	Si_soft00.usp	

Molecular dynamics

All the molecular dynamics simulations in this work are conducted with LAMMPS (Plimpton, 1995) simulation software. The interatomic interactions for these hydrated montmorillonite systems are simulated using CLAYFF (Cygan et al., 2004) force field which was chosen for its successful use in montmorillonite mineral simulations in the past (Greathouse & Cygan, 2005, Tao et al., 2010). The CLAYFF model differentiates an element into different types based on its structural position (tetrahedral or octahedral sheet and the neighbouring elements e.g. substitution sites) and assigns partial charges and van der Waals parameters to each atom type. It defines a bond stretch parameter for the structural hydroxyl groups and an angle bend parameter for the octahedral metal and OH. The interlayer water parameters in CLAYFF are from the flexible SPC (simple point charge) water model (Berendsen et al., 1981). Simulations were performed in the isothermal-isobaric (NPT) ensemble with three dimensional periodic boundary conditions. After a pre-equilibration the systems were equilibrated for 0.5 ns followed by the production run for another 0.5 ns at a temperature of 298 K and pressure 1 bar. A time step of 1 fs was used in the production run. To avoid translational drift of the clay layer, the centre of mass of the layer was fixed during the simulation. The data was recorded every 200 fs. The long range electrostatic interactions are calculated using Ewald summation

method (Karasawa & Goddard, 1989) with a precision of 1e-4. The short range electrostatic and van der Waals interactions are calculated using a 12.5 Å cut-off.

The initial montmorillonite structure for the simulations was obtained from QM calculations. Simulations were performed using three different layer charges for montmorillonite: -1.0 e/unit cell (x=1 i.e. 1 substitution per unit cell named later as Al3Mg1), -0.66 e/unit cell (x=0.66 i.e. 2 substitutions per 3 unit cells, named as Al10Mg2) and -0.5 e/unit cell (x=0.5 i.e. 1 substitution per 2 unit cells, named as Al7Mg1). The rectangular MD simulation box contains one clay lamellae and the interlayer with water and cations. The clay layer contains 4x4 unit cells measuring 20.7 Å x 35.8 Å (with layer charges -1.0 and -0.5 e/unit cell) or 6x3 unit cells measuring 31.1 Å x 26.9 Å (with layer charge -0.66 e/unit cell). Skipper et al. (1995) studied the effect of simulation box size and shape on the calculated interlayer properties and validated the use of a rectangular box containing eight unit cells (measuring 21.12 Å x 18.28 Å x 6.54 Å) of clay mineral. In this work, we chose to use a larger cell size in the xy-plane to insure the presence of multiple cations in each system. A snapshot of a rectangular Ca-montmorillonite simulation box is shown in Figure 1. Water content ranges from 1 to 16 molecules per unit cell (~0.02-0.4 g H_2O/g clay) in each case.

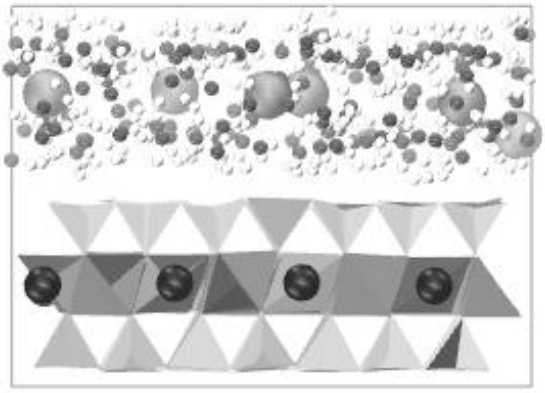

Figure 1 A snapshot of the MD simulation box: Si (tetrahedra), Al (octahedra), Mg (black), O (dark grey), H (white) and Ca (light grey).

These calculations consider only the equilibrium state of montmorillonite when water is forced into the interlayer. After the system is relaxed the mean value of the basal thickness (thickness of the layer and the interlayer) is obtained during the production run. The density profiles of interlayer atomic species are then derived in order to characterize the interlayer structure. Further, in order to consider diffusion coefficients for interlayer water, the mean squared displacement (msd) is calculated for water oxygens and cation species

$$< \Delta r^2(t) > = < |(r(t + t_0) - r(t_0)|^2 > \qquad (2)$$

averaging over all the considered atoms and all choices for the time origin t_0 from the recorded data (every 200 fs). The diffusion coefficient (D) is obtained from Einstein's relation

$$D = \lim_{t \to \infty} \frac{<\Delta r^2(t)>}{2d*t} \qquad (3)$$

where d is the dimensionality and t is time. As diffusion is limited perpendicular to the clay layer, the coefficients are obtained for diffusion parallel to the layer using the two dimensional Einstein equation.

RESULTS AND DISCUSSION

Structures

The target was for the calculated and experimental lattice parameters of the unit cell structures to be comparable so that the modelling results can be utilized

in order to interpret experimental findings. The lattice parameters from QM calculations for K-montmorillonite are presented in Table 1. Comparison of values indicates that the correspondence between the calculated and experimental parameters is good enough (Tsipursky & Drits, 1984; Bérend et al., 1995). The calculations were performed with different approximations. The main difference between the approximations is how energy states of the system are described, especially partial densities originated from p-orbitals.

Table 2. Calculated lattice parameters for K-montmorillonite.

	Exptl. [a]	GGA-PBE [b]	GGA-PBE [c]	GGA-PW91 [d]
a [pm]	518	499.7	529.4	529.1
b [pm]	897	870.8	908.1	909.2
c [pm]	995	1 047.6	1 084.5	1 095.8
α [°]	90.0	90.0	90.0	90.0
β [°]	99.5	101.2	101.4	104.5
γ [°]	90.0	90.0	90.0	90.0
d-value [pm]	981	1 027.6	1 063.0	1 060.9

[a] Tsipursky & Drits (1984).

[b] O_soft00.usp, Si_soft00.usp and Mg_00.usp.

[c] O_00PBE.usp, Si_00PBE.usp and Mg_00.usp.

[d] O_00PBE.usp, Si_00PBE.usp and Mg_00PW91.usp.

Na- and Ca-montmorillonite structures were generated by replacing K^+ ions with Na^+ ions in order to obtain Na-montmorillonite, and replacing a half of K^+ ions with Ca^{2+} ions and removing a half of K^+ ions in order to obtain Ca-montmorillonite. This way, the electrical neutrality of the structures remained. After that the structures were optimized, and the optimized parameters are presented in Table 3.

In montmorillonites, the equivalent amount of exchangeable cations depends on the amount of Mg(II) atoms replacing Al(III) in the negatively charged octahedral sheets. In the crystalline structure by Tsipursky and Drits (1984) for K-smectite, the Mg:Al ratio is 1:1. However, in montmorillonites the typical Mg:Al ratio is 1:5. In order to take into account the Mg:Al ratio in our studies and to remain the electrical neutrality of the models the unit cell structures (Figure 2a) had to be multiplied three times (1x3x1 unit cells). In these models, the positions of magnesium were selected so the distance between the magnesium atoms is as long as it is possible based on the symmetry. This selection corresponds rather closely the earlier published results by Lavikainen et al., 2015. These new periodic models (Figure 2b) were reoptimized and the optimized parameters for K-, Na- and Ca-montmorillonites are presented in Table 3.

Table 3. Calculated lattice parameters for K-, Na- and Ca-montmorillonites: a unit cell (1x1x1) with 1:1 Mg:Al ratio and a threefold cell (1x3x1) with 1:5 Mg:Al ratio. Note: no water present.

	K		Na		Ca	
	1x1x1	1x3x1	1x1x1	1x3x1	1x1x1	1x3x1
a [pm]	499.7	525.7	501.2	525.8	501.1	525.5
b [pm]	870.8	2 719.7	875.2	2 723.3	869.2	2 721.2
c [pm]	1 047.6	1 130 .0	1 161.3	1 087.5	1 023.8	1 049.2
α [°]	90.0	90.0	90.0	91.0	90.0	89.9
β [°]	101.2	100.7	114.2	97.2	108.1	100.9
γ [°]	90.0	90.0	90.0	90.0	90.0	90.0
d-value [pm]	1 027.6	1 030.1	1 058.9	1 078.7	973.4	1 110.3

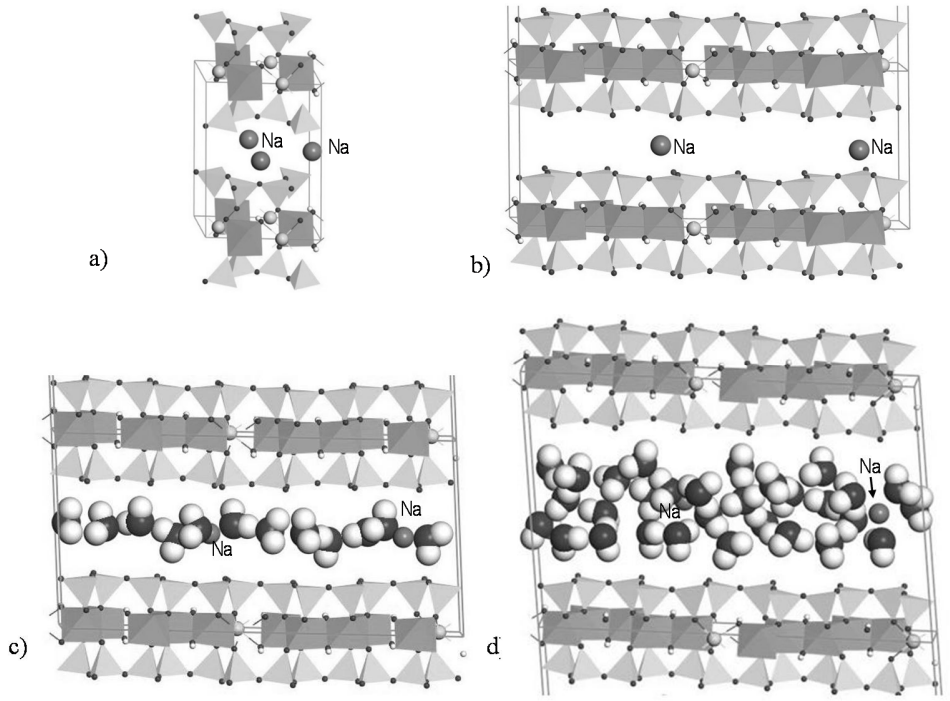

Figure 2 a) The unit cell of Na-montmorillonite from QM calculations, b) the model structure (1x3x1 unit cells) for MD simulations, and Na-montmorillonite with c) four and d) ten water molecules per the unit cell. Tetrahedral sheet: silicon. Octahedral sheet: aluminium. Spheres in octahedral sheet: magnesium. Small spheres in octahedral and tetrahedral sheets: oxygen. Interlayer: sodium and water.

Effect of water on structures

Typically the so-called dry montmorillonite contains about 8-10 wt-% water in its interlayer spaces. Based on the molecular mass of water and montmorillonite without interlayer water, the unit cell of the montmorillonite contains 2-4 water molecules. This means according to QM and MD simulations that only one water molecular layer exists in the interlayer space of the montmorillonite.

When the water content is over 10 wt-%, the interlayer space between the TOT layers starts to increase causing the swelling of the mineral. In this study, swelling was investigated with both QM and MD methods and QM was also used to detect possible atomic level changes in the structure of the TOT layers.

In the QM calculations, water content was varied from 0-10 water molecules in the unit cell corresponding to 0-246 mg H_2O / 1 g of montmorillonite. Water molecules were added randomly into the interlayer space of the montmorillonite models one by one and the structure was reoptimized between each step. A corresponding technique was used in the earlier work based on Monte Carlo simulations (Zheng et al., 2011). Na-montmorillonite structure with 98.2 mg H_2O / 1g montmorillonite (about 10 wt-%) is shown in Figure 2c, and its lattice parameters are a = 525.7 pm, b = 2 714.1 pm, c = 1 324.1 pm, α = 93.2°, β =

96.4°, γ = 89.9°, and d-value is 1 313.9 pm. Comparison to the parameters of the structure without water molecules indicates that the change of the lattice parameters is the most remarkable in the c axes direction increasing the distance (d-value) between the TOT layers. The water molecules appear as molecules in the interlayer space, and no reactions happen with the TOT layers. When there are 10 water molecules in the unit cell of the montmorillonite, the water content is about 24 wt-%, and the swelling is about 33% in the c direction (d-value = 1 747.6 pm) compared to the structure with 10 wt-% water. According to Figure 2d, at least two water molecular layers exist between the TOT layers. More detailed analysis of the swelling results together with those obtained from MD calculations is given later in the text.

Hydration of cations

Understanding the role of water on montmorillonite structures, the hydration of cations and clay layers has to be considered. Analysis of the coordination geometry of water molecules with cations reveals that free Na^+ has tetrahedral (Figure 3a) or octahedral (Figure 3b) coordination geometry with water molecules. Also free K^+ form four- or six-coordinated complexes with water (Figures 3c and 3d). The six-coordinated complex is trigonal prismatic. Free Ca^{2+} does not exist as a four-coordinated complex. It appears as an octahedral form

(Figure 3e) or eight-coordinated square antiprismatic form (Figure 3f). Hydration energies of Na^+, K^+ and Ca^{2+} cations are presented in Table 4. Earlier, Sposito et al. (1999) analyzed the coordination of the interlayer cations using Monte Carlo simulations.

Table 4. Hydration energies for Na^+, K^+ and Ca^{2+} cations.

	Hydration energy (kJ/mol)
$Na(H_2O)_4^+$	-397.73
$Na(H_2O)_6^+$	-534.24
$K(H_2O)_4^+$	-313.92
$K(H_2O)_6^+$	-458.81
$Ca(H_2O)_6^{2+}$	-1 123.96
$Ca(H_2O)_8^{2+}$	-1 294.24

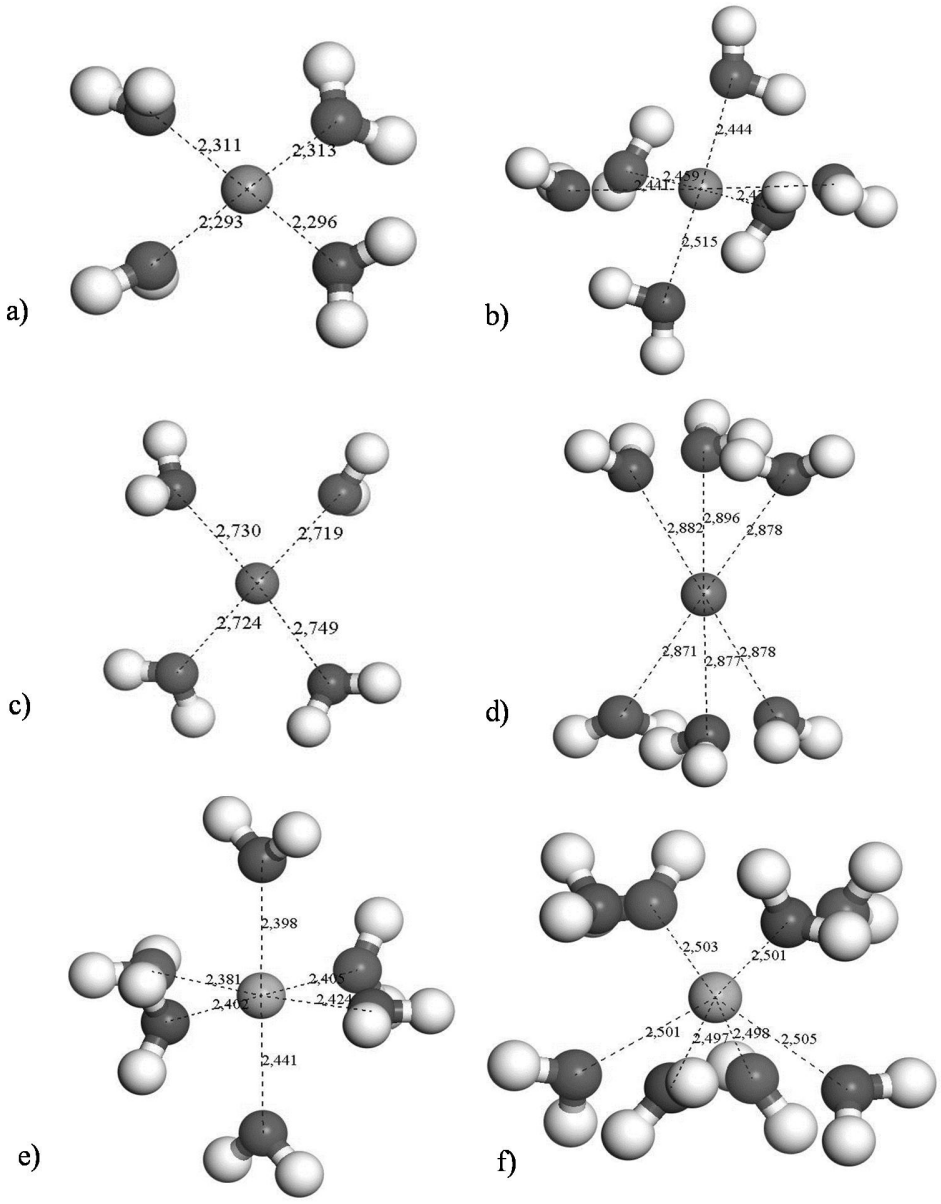

Figure 3 Cations coordination in montmorillonites based in QM calculations: a) four-coordinated Na^+, b) six-coordinated Na^+, c) four-coordinated K^+, d) six-coordinated K^+, e) six-coordinated Ca^{2+}, and f) eight-coordinated Ca^{2+}.

In the interlayer space of montmorillonites, cations also tend to achieve the corresponding coordination geometry like in their free form in water solutions. Our QM and MD simulations indicated that the interlayer water forms hydrogen bonds with the nearest cations and the oxygen atoms of the tetrahedral sheets. Na^+ has typically four water molecules in its coordination sphere, and further Na^+ can fulfil a part of its coordination sites by forming van der Waals bonding with the oxygen atoms of the tetrahedral sheet. K^+ favours asix-coordinated structure with five water molecules and one van der Waals bond to the tetrahedral sheet. Ca^{2+} also favours a six-coordinated complex, so there are three coordinated water molecules and three van der Waals bonds to the tetrahedral sheet. However, each of these structures varies case-by-case depending on the orientation of the randomly set water molecules in the interlayer space.

Swelling of montmorillonites relates to the strength of interaction forces of water molecules with other water molecules, cations and tetrahedral sheets within the interlayer spaces. This expansion process is controlled by the balance of attractive *vs* repulsive electrostatic forces resulting from the presence of negatively charged montmorillonite layers and interlayer cations. A variety of different intermolecular and electrostatic forces are valid, and these include hydrogen bonding, van der Waals forces, double layer repulsions and ion-ion correlation effects (Shirazi et al., 2011).

Due to Coulombic attractions between the negatively charged TOT layers and positively charged interlayer cations, the layers are initially held in close proximity to their neighbours. Van der Waals forces may also contribute to the total potential energy of attraction. The hydration energy of interlayer cations determines the total potential energy of repulsion, and thus the ease of penetration of water molecules into the interlayer space (Bérend et al., 1995). These sites remain closed until the expansion pressure of the surrounding water phase overcomes the resistance to interlayer space opening. This allows for a single layer of water molecules to enter and reside within the interlayer space, which in turn leads to a reduction in the potential energy of attraction as neighbouring layers are separated by a greater distance.

Following this initial phase, the hydration of interlayer cations may begin. The extent of cation hydration and swelling of montmorillonites is largely determined by the type of interlayer cations and their hydration energies (Bérend et al., 1995). In the case of the monovalent cations (Na^+, K^+) the degree of swelling is related to the hydration energy of the cations. However, hydration energies can vary significantly between different hydration degrees of cations (Table 4). Based on the greater hydration energies of the polyvalent cations (Ca^{2+}), the initial hydration happens faster than for the monovalent cations, because Ca^{2+} as a polyvalent cation can take up more water molecules into its coordination sphere

(up to eight water molecules) than Na^+ and K^+ as monovalent cations (Fig. 3). Because of this the hydrogen bonding of the Ca^{2+} cations with the tetrahedral sheet is stronger than that of the Na^+ and K^+ cations. In order to add additional water into the interlayer space, the free energy loss of the incoming water must be greater than the work done in increasing the interlayer space. Therefore, Na- and K-montmorillonites can take up more water than Ca-montmorillonite.

Swelling

The d-values of Na-, K- and Ca-montmorillonites with three different layer charges and varying interlayer water content were obtained from MD calculations where water was forced into the interlayer. The d-values are given together with the QM results (using layer charge -0.66 e per unit cell), XRD results from Fu et al. (1990) for Na-montmorillonite, Cases et al. (1997) for Ca-montmorillonite and Berend et al. (1995) for K-montmorillonite and MC results from Zheng et al. (2011) for Na-montmorillonite with respect to the interlayer water content in Figure 4. In each case, MD results indicate that montmorillonites with smaller layer charges experience greater swelling. However, in the case of K-montmorillonite the difference in swelling between the three structures is the smallest.

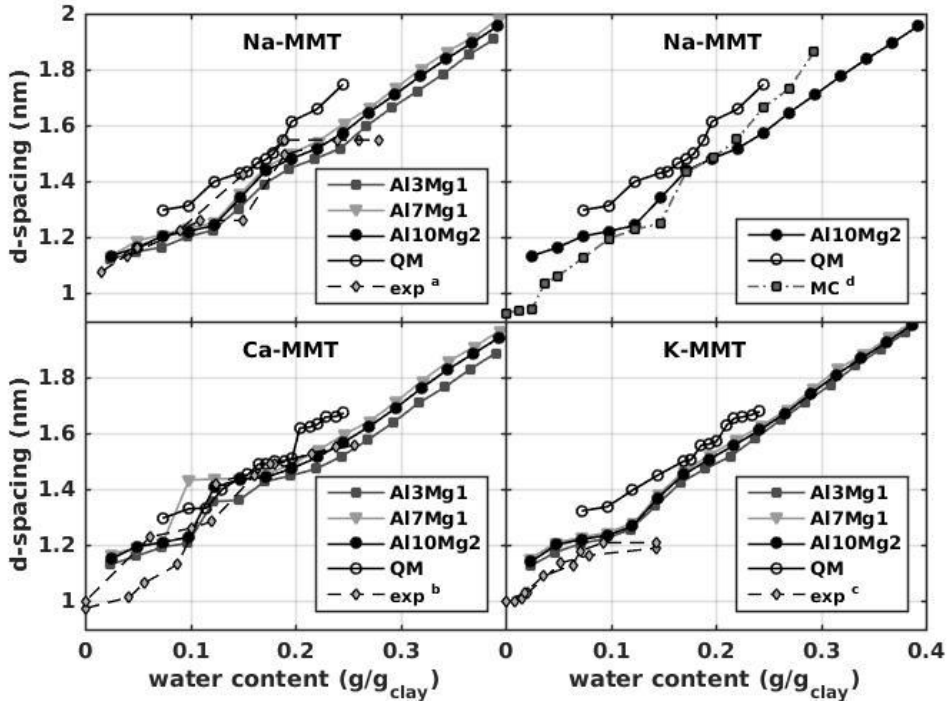

Figure 4 The Swelling curves of Na-, Ca- and K-montmorillonites with different layer charges from MD and QM studies (Note: water is forced into the interlayer) and experimental results a) Fu et al. (1990), b) Cases et al. (1997), c) Berend et al. (1995) and MC calculations Zheng et al. (2011).

Comparison of the MD results for Na-, Ca- and K-montmorillonites with the same layer charges and water contents shows that generally K-montmorillonite exhibits the largest d-value with the exception of Ca-montmorillonite in the water content range of about 0.1-0.15 g/g. This Ca-result is consistent with the findings based on the hydration energies of different cations (Table 4) and is also supported by the XRD results. Denis et al. (1991) reported the influence of K in montmorillonite as a swelling inhibitor which is not observed in these results because water is forced into the interlayer (note the absence of external water). QM results indicate that Na-montmorillonite exhibits the largest d-value above ~0.2g/g water content. Also, QM predicts larger d-values than MD, but in general similarities can be detected (the most for Ca-montmorillonite). The trends in swelling graphs are in general agreement with the results from XRD and MC (for Na-montmorillonite). Differences in the experimental and simulation results are possibly due to the differences in the structures, like the presence of tetrahedral substitutions in the experimental samples.

Interlayer structures

Examples of density distributions of the interlayer water oxygens and cations for Na-, Ca- and K-montmorillonites (layer charge 0.5 e per unit cell) are presented in Figures 5, 6 and 7, respectively. In these plots, x-axis is the basal

distance from the bottom of the clay layer to the top of the interlayer space and the clay layer thickness is about 0.64 nm (calculated from atom centre to atom centre). All density curves of water oxygens show peaks indicating the formation of water layers. For some water contents these peaks are not as distinct (see Figure 5 bottom left hand corner). They are considered here as "mixed states" when the previously existing water layers are "full" and before the formation of yet another clearly separate layer is favourable. For Na-montmorillonite we can observe that the second water layer starts to form when water content is increased to 6 molecules per unit cell and the third layer begins to form at water contents 10-11 molecules per unit cell. These regions are represented by a step in the swelling graphs in Figure 4. For Ca-montmorillonite we observed that two water layers began to form when water content was increased to 4-5 molecules per unit cell and three water layers with 13-14 water molecules per unit cell. For K-montmorillonite two water layers started to form when water content was increased to 6 molecules per unit cell and three water layers with 12 water molecules per unit cell.

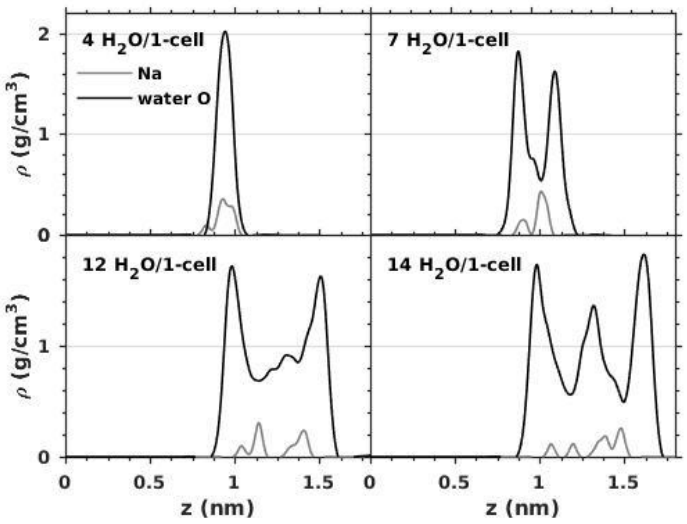

Figure 5 Density distributions (from MD) of interlayer species for Na-montmorillonite (Al7Mg1) with interlayer water contents 4, 7, 12 and 14 molecules/unit cell.

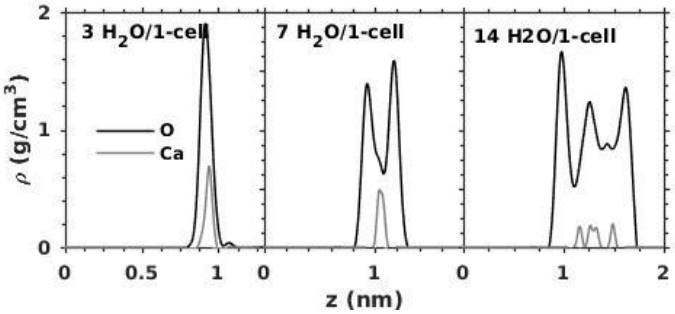

Figure 6 Density distributions (from MD) of interlayer species (water oxygen and cation) for Ca-montmorillonite (Al7Mg1) with interlayer water contents 3, 7 and 14 molecules/unit cell.

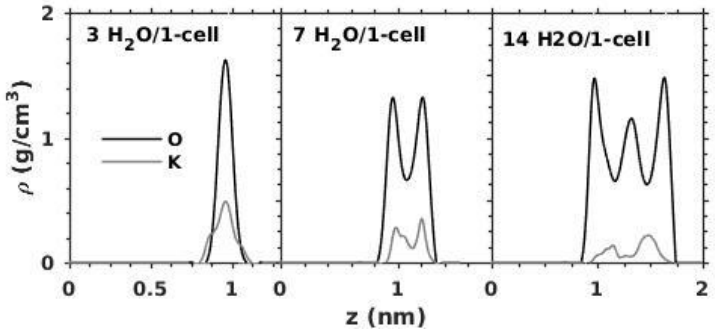

Figure 7 Density distributions (from MD) of interlayer species (water oxygen and cation) for K-montmorillonite (Al7Mg1) with interlayer water contents 3, 7 and 14 molecules/unit cell.

The density distributions of Na in the plots in Figure 5 indicate that the cations are surrounded by water molecules for the majority of water contents, exception being in the lower water contents. The same behaviour is demonstrated by Ca-montmorillonite (see Figure 6). However, K cations are distributed more uniformly in the interlayer space as can be seen from Figure 7 indicating that they are not “bound” between water layers.

The radial distribution functions (RDF) of cation-water oxygens for one, two and three layer hydrates are presented in Figure 8 for Na- and Ca-montmorillonites with layer charge -0.5 e/unit cell and K-montmorillonite with layer charge -1.0 e/unit cell. For Na-montmorillonite the first neighbour peak is found around 0.23-0.24 nm in each hydrate case. For Ca-montmorillonite this peak is found around 0.24-0.25 nm. K-montmorillonite gives the peak at around 0.28-0.29 nm in each case. Similar results were obtained by Tao et al. (2010). The RDFs of water oxygen-water oxygen for the corresponding cases are shown in Figure 9. In each case the first neighbour peak is around 0.27-0.28 nm. However, the three layer hydrate peak for Ca case is found to be slightly shifted when compared to the other two states.

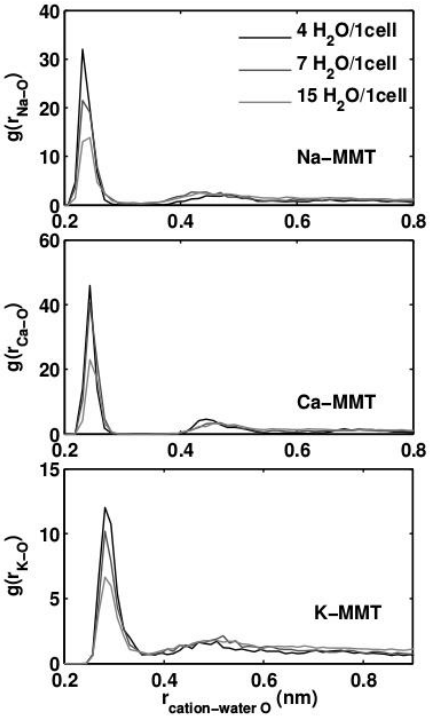

Figure 8 RDF (from MD) for cation-water oxygen atoms for Na- and Ca-montmorillonites with layer charge -0.5 e/unit cell and K-montmorillonite with layer charge -1 e/unit cell.

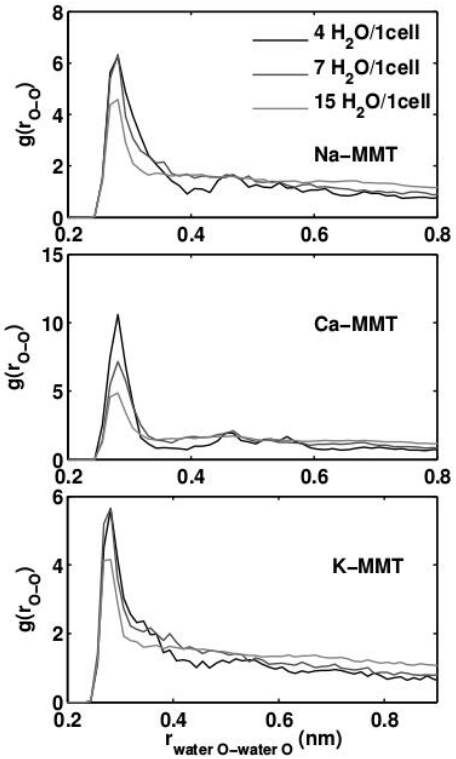

Figure 9 RDF (from MD) for water oxygen-water oxygen atoms for Na- and Ca-montmorillonites with layer charge -0.5 e/unit cell and K-montmorillonite with layer charge -1 e/unit cell.

Diffusion of water and cations

The MSDs of interlayer water (oxygens) and cations for Na-, Ca- and K-montmorillonites (Al10Mg2) with 10 H_2O/unit cell are given as a function of time in Figure 10. According to Einstein's relation the slope of the MSD curve gives a quantitative measure of the diffusion coefficient. The statistics of the time correlation data deteriorate after half length of the 500 ps run and especially for cations the statistics suffer from using a small number of particles, as can be seen in Figure 10. To obtain the slope, a least-squares fit is done to 40-80 % of the data up to 250 ps.

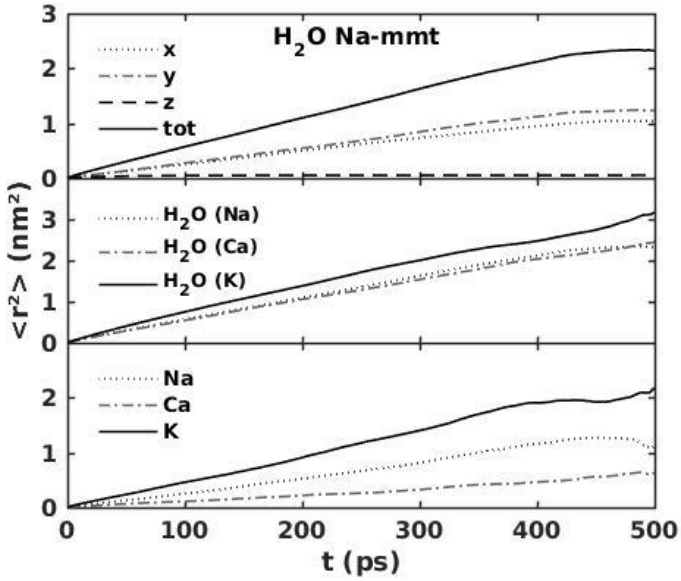

Figure 10 MSD from MD calculations: x, y, z and total components for interlayer water in Na-montmorillonite with 10 H_2O/unit cell (top), interlayer water (O) in Na-, Ca and K-montmorillonites with 10 H_2O/unit cell (middle) and the interlayer cations (bottom).

The values of the diffusion coefficients obtained for water and cations are presented together with the MD results from Holmboe & Bourg (2014), Greathouse et al. (2015) and Boek (2014) (results reported for 3D diffusion and, thus, are lower than 2D values) in Figures 11 and 12, respectively. Note however, that calculating the diffusion coefficients for cations suffer from using small numbers of particles and, thus, only the values for montmorillonites with the larger layer charges (-0.66 and -1.0 e/unit cell) are reported. In general, the values increase with increasing water content and with decreasing layer charge. However, the rise is not linear. A rapid increase is observed in the values from monohydrate to bi-hydrate montmorillonite, and as the water content is increased from approximately half saturated hydrate structure to fully saturated, the values of the diffusion coefficients decrease. In general, diffusion in Ca-montmorillonite is slower than in both Na- and K-montmorillonites which is likely due to the different coordination and stronger interaction of the divalent Ca^{2+} versus the monovalent Na^{+} or K^{+}. The results are in satisfactory agreement with those from previous MD studies considering the different structures used.

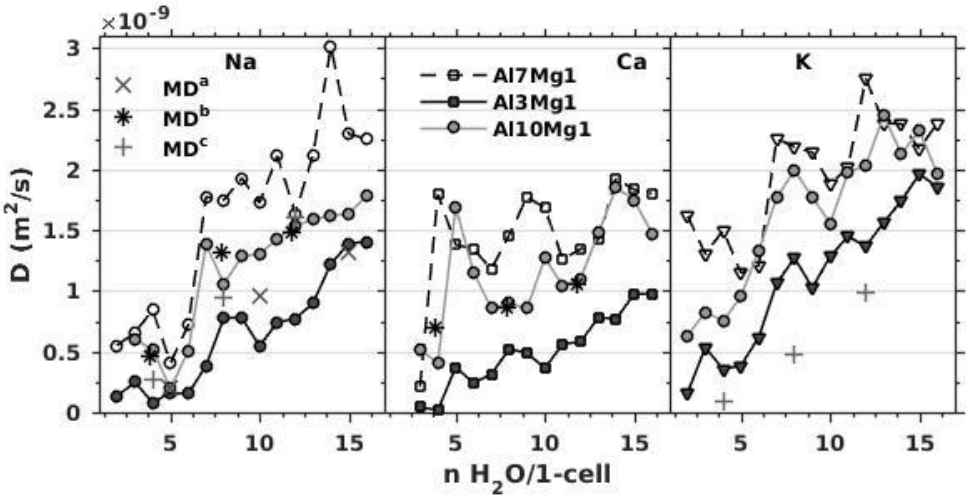

Figure 11 The 2D interlayer water self-diffusion coefficients (from MD) for Na-, Ca- and K-montmorillonites and the MD results from a) Holmboe & Bourg (2014), b) Greathouse et al. (2015) and c) Boek (2014) (given in 3D).

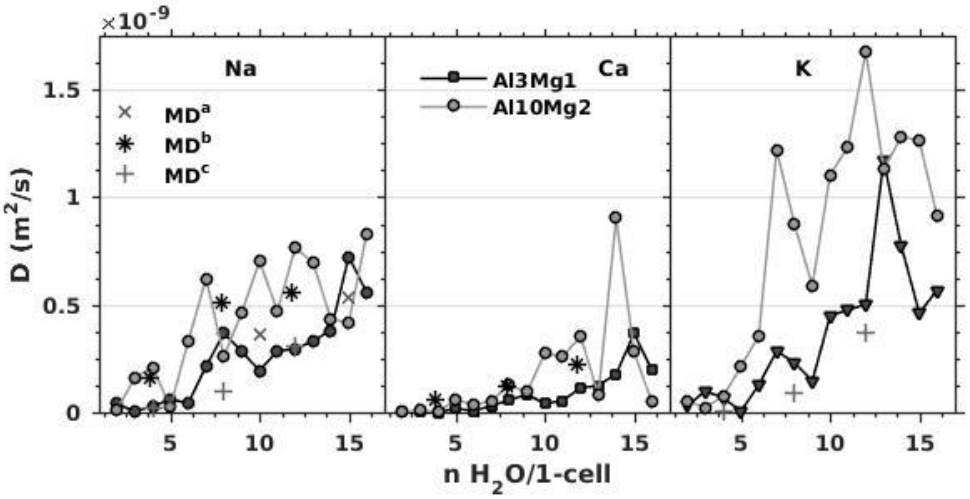

Figure 12 The 2D interlayer cation self-diffusion coefficients (from MD) for Na-, Ca- and K-montmorillonites and the MD results from a) Holmboe & Bourg (2014), b) Greathouse et al. (2015) and c) Boek (2014) (given in 3D).

CONCLUSIONS

This study indicated that both QM and MD can be used to study the swelling of montmorillonites. Based on the results for montmorillonites with only octahedral substitutions, smaller layer charge results in greater swelling, and the type of cation present in the interlayer also has a remarkable effect on the swelling properties. MD simulations indicated that generally K-montmorillonite exhibits the largest d-value though the difference in the d-value of different K-montmorillonites was the smallest. The modelled swelling behaviour of K-montmorillonite contradicts the experimental observations where K acts as a swelling inhibitor. This is a result of the system setup. The simulations considered only the equilibrium state of a montmorillonite system where water is forced into the interlayer and the rate with which water is adsorbed is not taken into account. Similarities between the MD and QM results were detected, though in general QM predicts d-values larger than MD. The probable reason is that QM calculations are static, and movement of atoms has not been taken into account as a function of time. Based on the MD calculations, the formation of water layers in the interlayer space of the montmorillonites which is well known for natural samples could be reproduced.

The data from MD calculations was also used to predict the self-diffusion coefficients of interlayer water and cations. It was found that the coefficient is

not constant but increases nonlinearly with increasing water content and with decreasing layer charge.

In the future, cation exchange reactions of montmorillonites in different salt concentrations should be studied in order to better describe the transport behaviour of water and cations in (and to) the interlayer space of montmorillonites. However, hydration energies of cations in the interlayer space of montmorillonites and swelling pressures cannot be predicted based on these results.

Conclusion of the present work is that QM/MD techniques together are relevant methods to study nanolevel interactions which determine macroscopic phenomena related to montmorillonites. Further, in order to develop reliable continuum mechanics models, nanolevel data is needed to select relevant data into these models.

ACKNOWLEDGEMENTS

The authors wish to acknowledge funding received from Posiva Oy.

NOMENCLATURE

CASTEP	Cambridge serial total energy package
DNP	Double Numerical plus Polarization
GGA-PBE	Perdew, Burke and Ernzerhof version of generalized gradient approximation functional
GGA-PW91	Generalized gradient approximation (Perdew-Wang)
MD	Molecular dynamics
O	Octahedral
QM	Quantum mechanics
T	Tetrahedral

REFERENCES

Accelrys (2011) *MS Modeling, Release 6.0*. San Diego: Accelrys Software Inc.

Accelrys (2013) *MS Modeling, Release 7.0*. San Diego: Accelrys Software Inc.

Berend, I., Cases, J. M., Francois, M., Uriot, J. P., Michot, L., Maison, A. & Thomas, F. (1995) Mechanism of adsorption and desorption of water vapor by homoionic montmorillonites: 2. The Li^+, Na^+, K^+, Rb^+ and Cs^+-exchanged forms. *Clays and Clay Minerals*, **43**, 324-336.

Berendsen, H. J. C., Postma, J. P M., van Gunsteren & W. F., Hermans, J. (1981) Interaction models for water in relation to protein hydration. Pp. 331-342 in: *Intermolecular forces* (B. Pullman, editor). D. Reidel Publishing, Dordrecht.

Boek, E. S. (2014) Molecular dynamics simulations of interlayer and mobility in hydrated Li-, Na- and K-montmorillonite clays. *Molecular physics*, **112**, 1472-1483.

Brigatti, M. F., Galan, E. & Theng, B. K. G. (2006) Structures and mineralogy of clay minerals. Pp. 19-86 in: Handbook of Clay Science, (Developments in Clay Science), Volume 1. Elsevier Ltd., Amsterdam.

Cases, J.M., Berend, I., Francois, M., Uriot, J.P., Michot, L.J. & Thomas, F. (1997) Mechanism of adsorption and desorption of water vapor by homoionic montmorillonites: 2. The Mg^{2+}, Ca^{2+}, Sr^{2+} and Ba^{2+}-exchanged forms. *Clays and Clay Minerals*, **45**, 8-22.

Chatterjee, A., Iwasaki, T., Ebina, T. & Miyamoto, A. (1999) A DFT study on clay-cation-water interaction in montmorillonite and beidellite. *Computational Materials Science*, **14**, 119-124.

Clark, S.J., Segall, M.D., Pickard, C.J., Hasnip, P.J., Probert, M.J., Refson, K. & Payne M.C. (2005) First principles methods using CASTEP. *Zeitschrift fuer Kristallographie*, **220**, 567-570.

Cygan R.T., Liang, J.-J. & Kalinichev, A.G. (2004) Molecular models of hydroxide, oxyhydroxide, and clay phases and the development of a general force field. *Journal of Physical Chemistry B*, **108**, 1255-1266.

Denis, J. H., Keall, M. J., Hall, P. L. & Meeten, G. H. (1991) Influence of potassium concentration on the swelling and compaction of mixed (Na, K) ion-exchanged montmorillonite. *Clay Minerals*, **26**, 255-268.

Dohrmann, R., Kaufhold, S., Lundqvist, B. 2013. The Role of Clays for Safe Storage of Nuclear Waste. Pp. 677–710 in: Developments in Clay Science, Vol. 5B, Handbook of Clay Science, Techniques and Applications (F. Bergaya and G. Lagaly, editors). Elsevier, Amsterdam.

Ebina, T., Iwasaki, T., Onodera, Y. & Chatterjee (1999) A comparative study of DFT and XPS with reference to the adsorption of caesium ions in smectites. *Computational Materials Science*, **14**, 254-260.

Fu, M. H., Zhang, Z. Z. & Low, P. F. (1990) Changes in the properties of a montmorillonite-water system during the adsorption and desorption of water: hysteresis. *Clays and Clay Minerals*, **38**, 485-492.

Greathouse, J. A. & Cygan, R. T. (2005) Molecular dynamics simulation of uranyl(VI) adsorption equilibria onto an external montmorillonite surface. *Physical Chemistry Chemical Physics*, **7**, 3580-3586.

Greathouse, J. A., Cygan, R. T., Fredrich, J. T. & Jerauld, G. R. (2015) Molecular dynamics simulation of diffusion and electrical conductivity in montmorillonite interlayers. *The Journal of Physical Chemistry C*, **120**, 1640-1649.

Hattori, T., Saito, T., Ishida, K., Scheinost, A.C., Tsuneda, T., Nagasaki, S. & Tanaka, S. (2009) The structure of monomeric and dimeric uranyl adsorption complexes on gibbsite: A combined DFT and EXAFS study. *Geochimica et Cosmochimica Acta*, **73**, 5975-5988.

Holmboe, M. & Bourg, I. (2014) Molecular dynamics simulations of water and sodium diffusion in smectite interlayer nanopores as a function of pore size and temperature. *The Journal of Physical Chemistry C*, **117**, 1001-1013.

Karasawa, N. & Goddard, W., A. (1989) Acceleration of convergence for lattice sums. *Journal of Physical Chemistry*, **93**, 7320-7327.

Lavikainen, L.P., Tanskanen, J.T., Schatz, T., Kasa, S. & Pakkanen T.A. (2015) Montmorillonite interlayer surface chemistry: effect of magnesium ion substitution on cation adsorption. *Theoretical Chemistry Accounts,* 134, 2-7.

Leach, A.R. (2001) *Molecular Modelling, Principles and Applications*, 2nd ed., Pearson Education Limited, Essex.

Murray, H. H. (2000) Traditional and new applications for kaolin, smectite, and palygorsgyte: a general overview. *Applied Clay Science,* **17**, 207-221.

Plimpton, S.J. (1995) Fast parallel algorithms for short-range molecular dynamics. *Journal of Computational Physics*, **117**, 1-19.

Ren, X., Yang, S., Tan, X., Chen, C., Sheng, G. & Wang, X. (2012) Mutual effects of copper and phosphate on their interaction with γ-Al_2O_3: Combined batch macroscopic experiments with DFT calculations. *Journal of Hazardous Materials*, **237-238**, 199-208.

Rotenberg, B., Marry, V., Salanne, M., Jardat M. & Turq, P. (2014) Multiscale modelling of transport in clays from the molecular to the sample scale. *Comptes Rendus Geoscience*, **346**, 298-306.

Rowe, R. K., Quigley, R. M. & Booker, J. T. (1997) *Clayey barrier systems for waste disposal facilities.* E & FN Spon, London.

Shirazi, S. M., Wiwat, S., Kazama, H., Kuwano. & Shaaban. M. G. (2011) Salinity effect on swelling characteristics of compacted bentonite. *Environment Protection Engineering*, **37**, 65-74.

Skipper, N. T., Chang, F.-R. C. & Sposito, G. (1995) Monte Carlo simulations of the interlayer molecular structure in swelling clay minerals. 1. Methodology. *Clays and Clay Minerals*, **43**, 285-293.

Sposito, G., Skipper, N.T.,Sutton, R., Park, S.-H. Soper, A.K. & Greathouse, J.A. (1999) Surface geochemistry of the clay minerals. *Proceedings of the National Academy of Sciences*, **96**, 3358-3364.

Tambach, T.J., Hensen, E.J.M. & Smit, B. (2004) Molecular simulations of swelling clay minerals. *Journal of Physical Chemistry B*, **108**, 7586-7596.

Tao, L., Xiao-Feng, T., Yu, Z. & Tao, G. (2010) Swelling of K^+, Na^+ and Ca^{2+} - montmorillonites and hydration of interlayer cations: a molecular dynamics simulation. *Chinese Physics B*, **19**, 109101(1-7).

Tribe, L., Hinrichs, R. & Kubicki, J.D. (2012) Adsorption of Nitrate on Kaolinite Surfaces: A Theoretical Study. *The Journal of Physical Chemistry B*, **116**, 11266-11273.

Tsipursky, S.I.& Drits, V. A. (1984) The distribution of octahedral cations in the 2:1 layers of dioctahedral smectites studied by oblique-texture electron diffraction. *Clay Minerals*, **19**, 177-193.

Velde B. & Meunier A. (2008) The origin of clay minerals in soils and weathered rocks. Springer-Verlag, Berlin Heidelberg.

Viani, A., Gualtieri, A.F. & Artioli, G. (2002) The nature of disorder in montmorillonite by simulation of X-ray powder patterns. *American Mineralogist*, **87**, 966-975.

Wesolowski, D.J., Bandura, A.V., Cummings, P.T., Fenter, P.A., Kubicki, J.D., Lvov. S.N., Machesky, M.L., Mamontov, E., Předota, M., Ridley, M.K., Rosenqvist, J., Sofo, J.O., Vlcek, L. & Zhang, Z. (2009) Atomistic origins of mineral-water interfacial phenomena and their relation to surface complexation models. *Geochimica et Cosmochimica Acta*, **73(13)**, A1429.

Zheng, Y., Zaoui, A. & Shahrour (2011) A theoretical study of swelling and shrinking of hydrated Wyoming montmorillonite. *Applied Clay Science*, **51**, 177-181.